

Comparative Analysis of Integer and Fractional PID for Power Regulation Integrated in an Electrosurgical Generator

Hussban Abood Saber, Ali Jafer Mahdi*, Manal Hussein Nawir

Department of Electrical and Electronics Engineering, University of Kerbala, Karbala, Iraq.

* Corresponding author, Email: ali.j.mahdi@uokerbala.edu.iq

Received: 29 October 2021; Revised: 12 December 2021; Accepted: 14 December 2021

Abstract

The electrosurgical generator (ESG) unit must be adapted to satisfy tissue impedance unpredictability while supplying power. The body's impedance changes complicate power supply and voltage control. ESG relies on output power in the constant power range. This study's goal is to supply active power that varies with tissue impedance. The impedance tissues are represented as a parallel RC circuit with three models (Child, Male, and Female). To enhance ESGs performance, integer-order PID (IO-PID) and fractional order PID (FO-PID) controllers are designed for controlling the output power and voltage. The particle swarm optimization (PSO) method is used to optimize IO-PID and FO-PID controllers' gains. Two control systems are compared in terms of overshoot, undershoot, rise and settling times, and steady-state error. It is concluded that FO-PID-based ESG is more robust and efficient compared with IO-PID-based ESG.

Keywords: electrosurgical generator, bio-impedance tissue, integer order-PID, fractional order-PID, particle swarm optimization

1. Introduction

Electrosurgical technology has been used for over a century. However, some issues still exist. The active power given to the patient tissue should be measured to allow for quick feedback and power management. In a standard feedback control scheme, PID controllers have been effectively used. The primary reason for this is that they are simple in their application and understanding. PID controllers do

not always control nonlinear, unpredictable, and interconnected systems effectively. As a result, it lacks the ability to reject disturbances and is usually ineffective. Many academics have tried to improve PID controller performance by creating new architectures and tuning methods. Podulbny introduced a new type of controller called a fractional order PID (FO-PID) in 1999 [1]. Recently, scientists and engineers have been attracted to the use of fractional calculus and PID control theory to create FO-PID controllers. The FO-PID controller is used in many practical applications, such as aerospace control systems, motion control of manipulators, heat diffusion systems, control of military thermal systems, electric power systems, and varying time-delay processes [2]. Additional tuning options are available on FO-PID controllers. As a result, FO-PID controllers provide designers with more flexibility, requiring them to address specific constraints such as iso-damping. High-order integrators improve tracking but reduce closed system stability. while High order differentiators have limited stability margins and closed-loop noise rejection. The FO-PID controller can be a good trade-off among IO-PID controllers like PI^2D , PID^2 , and PI^2D^2 . In other words, FO-PID is a trade-off between increased precision (higher integrator order) and increased stability (higher differentiator order). As a result, depending on the performance requirements, FO-PID controllers may outperform IO-PID controllers [3]. Designing IO-PID and FO-PID controllers requires reasonable parameter tuning. Each of these parameters must be optimised to produce optimal controllers. A strong intelligent strategy for improving controller parameters, Particle Swarm Optimization (PSO) is used. It is a simple and low-cost algorithm [4].

Several researchers have conducted studies on the electrosurgical generator's performance. To keep the power delivery and voltage within acceptable ranges, PIDSMC (Proportional Integral Derivative Sliding Mode Control) was utilised [5]. The ESU's output power was regulated to a fixed value using a fuzzy logic controller (FLC) adjusted proportional integral derivative (PID) controller [6] in a fully closed-loop control method. In the constant power area, robust fractional-order control is evaluated with fixed and variable tissue impedance [7]. These studies showed good results in terms of maintaining ESG output, but it focused exclusively on one issue, namely improving the generator's properties. They did not address other issues. For example, the ESG has not investigated over a wide frequency range; rather, the research concentrated on a single frequency. Furthermore, the generator's hardware components have not studied in their non-ideal state, but rather the majority of these studies ignored the practice conditions. These studies did not employ a variety of load types to determine the influence of variable tissue impedance on the ESG's performance. In [8], the ESG's performance was evaluated throughout a frequency range of 10 kHz to 1 MHz and with a non-ideal buck converter unit.

From an economic standpoint, a 96.51 % efficiency at 100 kHz has been obtained. Moreover, three different loads (e.g. based on age and gender) have been used. The ESG's power has not regulated to the specified value. The controller of the ESG does not include an intelligent control mechanism for adjusting the amount of variable output power in response to tissue impedance changes [8]. As a result, this study aims to develop advanced power controllers for the ESG that produce a constant output power regardless of the load. This study relies on [8] for the analytical examination of the generator's hardware components, as the buck converter circuit was analysed at a frequency of 100 kHz and the inverter circuit was designed at a frequency of 500 kHz, as well as the use of three different types of loads arranged in multiple layers. A robust and closed control system is constructed using IO-PID and FO-PID controllers, the parameters of which are modified using the PSO method to determine the optimal values for each controller's parameters. The performance of the ESG is compared to that of IO-PID and FO-PID controllers in each layer that comprises the tissues, based on their transient response characteristics.

2. Electrosurgical generator (ESG)

Electrosurgery is a technique in which high-frequency currents are used to perform clinical procedures such as fulguration, desiccation, and cutting on the human body. Tissue in the exposed area will suffer i^2R heating when a high-frequency current is delivered to the human body. The tissue will react differently depending on the temperature reached. The body has resistance to current flow. As a result, the entire exposed zone will be included in the circuit. As the cutting depth grows, so it resists this current, which is delivered to the tissue via an electrode. When current-carrying electrodes contact tissue, the current flows throughout the tissue. The current density increases with proximity to the electrode. Figure1 shows the electrosurgery procedure [9].

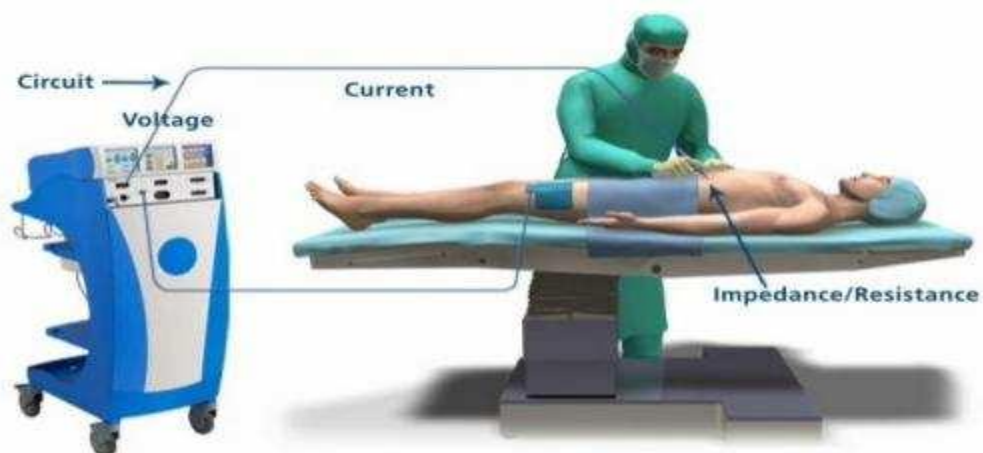


Figure 1 A typical electrosurgical procedure.

The voltage is supplied by an ESG. An ESG is a device that takes electrical energy from the mains and converts it into a high frequency (HF) current. Figure 2 shows the main components of an ESG which are as follows. Rectification is the initial stage, in which alternating current is converted to direct current. The magnitude of the DC-rectified voltage signal is reduced by a buck converter in the second stage. In the third stage, the inverter converts the direct current signal to high power, high frequency alternating current signal. A high-frequency transformer couples the inverter's output to the probe during surgical procedures [7]. details of the ESG design, as well as the loads used in this study, can see in the research [8]. Parameters of the buck converter, H-bridge inverter and loads, used in our study are given in Tables 1,2 and 3, respectfully.

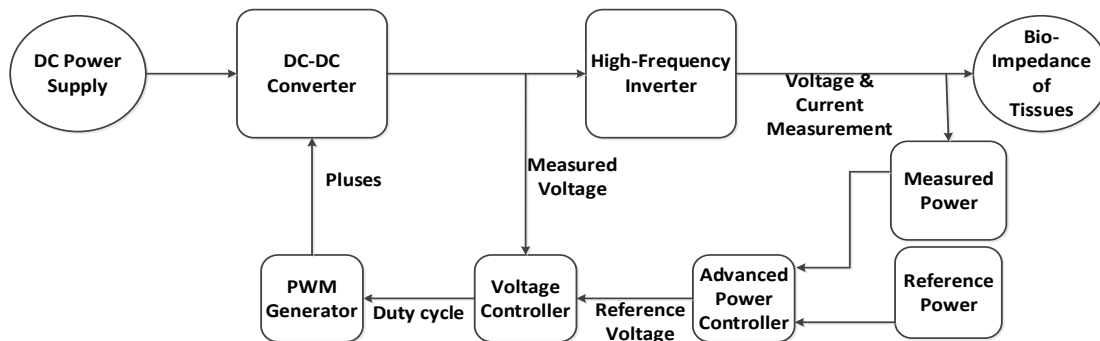


Figure 2 Block diagram of the electrosurgical generator.

Electrosurgery is commonly used in reproductive surgery, and technical developments have improved efficacy and reduced potential consequences [10]. Reduced blood loss, dry and quick tissue separation, and a lower risk of cutting harm to surgeons are some of the possible advantages of electrosurgery [11]. However, according to the Association of perioperative Registered Nurses, malfunctioning electrosurgical devices cause over 40000 patients to burn instances in the United States each year [12]. The reason for this is that tissue impedance varies, and ESG output power is dependent on tissue impedance. Because of the delayed response of the circuit in the ESG to changes in impedance, output power fluctuates during arching, resulting in tissue charring. To avoid charring, a sophisticated control system, as illustrated in Fig. 2, must be built to manage output power and peak voltage in a way that helps to achieve constant power properties.

Table 1 Buck converter design specifications.

Description	Value, Unit
Input Voltage	24 V
Switching Frequency	100 kHz
Inductor	67.14 μ H
ESR of Inductor	68.84 m Ω
Capacitor	22 μ F
ESR of Capacitor	0.60 Ω
Current Ripple	0.62 A
Voltage Ripple	60 mV
Efficiency	96.51 %

Table 2 H-bridge inverter design specifications.

Description	Value, Unit
Input Voltage	6 V
Output Voltage	120 V
Reference Power	100 W
Transformer Turns Ratio	1:20
Efficiency of Transformer	94 %
Switching Frequency	500 kHz

Table 3 Bio-impedance tissues design specifications [8].

Model	Age (years)	Organs	Resistance (Ω)	Capacitance (pF)
Child	7	Skin	15.27	86.06
		Muscle fat average	26.88	31.88
		Nerve	14.78	83.67
Male	38	Skin	50.36	50.50
		Fat	500.15	6.45
		Muscle	42.39	19.46
		Nerve	29.57	41.83
Female	40	Skin	20.36	64.54
		Fat	344.35	4.30
		Muscle	35.33	23.35
		Nerve	22.18	55.78

3. PID controllers

3.1 Integer Order-PID Controller (IO-PID)

Most industrial applications are using classical, integer-order type PID controllers due to the widely known characteristics such as simplicity, the existence of tuning methods based on the process model, and the provided robustness performances [13]. IO-PID controller consists of three types of control i.e., Proportional, Integral, and Derivative control as shown in Fig. 3.

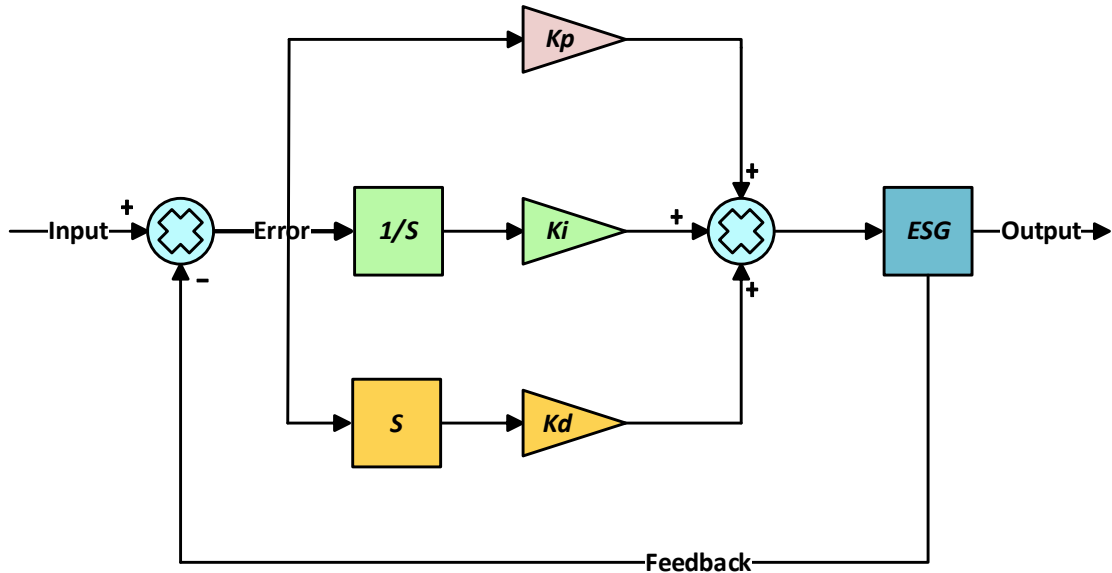


Figure 3 IO-PID controller.

The system transfer function in the continuous s-domain is given as following.

$$G_{IO-PID}(S) = K_p + \frac{K_i}{S} + K_d S \quad (2)$$

where K_p is the proportional gain, K_i is the integration coefficient and K_d is the derivative coefficient. K_p , K_i , and K_d all affect the performance of a PID controller. These gains can be obtained by employing the Ziegler-Nichols method, gain-phase margin, Root Locus, Minimum Variance, and Gain Scheduling; however, these methods are not optimal for nonlinear and high-order control systems, and some methods are quite difficult. The particle swarm optimization (PSO) approach is presented to overcome these constraints and obtain optimal K_p , K_i , and K_d . PSO is recommended since it produces convergent results and does not necessitate many iterations.

3.2 Fractional Order-PID Control (FO-PID)

Today, fractional-order proportional integration derivative (FO-PID) controllers have attracted much attention from academia and industry. Despite FO-PID controllers outperforming integer order (IO) ones in many cases, the latter continues to dominate industrial utilization [3] [14]. The main difference between IO-PID and FO-PID is the non-integer orders of derivative and integral parts. The FO-PID controller has two extra parameters, λ , and μ , which make the controller more adaptable [15], as shown in Fig. 4.

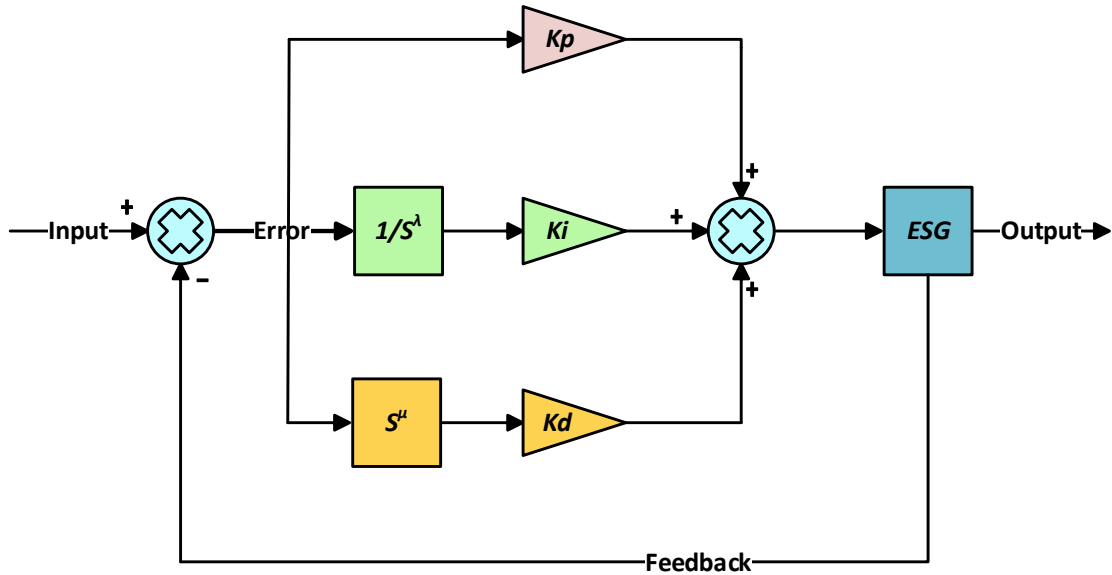


Figure 4 FO-PID controller.

The system transfer function in the continuous s-domain is given as following

$$G_{FO-PID}(S) = K_p \left(1 + \frac{K_i}{S^\lambda} + K_d S^\mu \right) \quad (3)$$

where λ and μ are the orders of integration and differentiation respectively allowed to be non-integer positive numbers, where, λ and μ value should be $0 < \lambda, \mu < 1$ and when taking $\lambda=1$ and $\mu=1$, we will have an integer-order PID controller [16]. Five parameters must be properly tuned to construct a controller $(K_p, K_i, K_d, \lambda, \mu)$. The ideal set of these parameters must be found to provide the best controller. Tuning these five parameters has become a popular issue that has been explored and optimized by various powerful intelligent procedures such as Nelder-Mead (NM) method, Genetic Algorithm (GA), Zeigler-Nichols (ZN) method, Artificial Bee Colony (ABC) algorithm, and Particle Swarm Optimization (PSO) algorithm. In this study, the PSO technique is recommended for obtaining the best FO-PID parameter values.

4. PSO algorithm

PSO is a developmental arithmetic algorithm invented by Kennedy and Elberhat in 1995 [17]. Essentially, this algorithm works on the traditional behavior of a flock of birds. This algorithm is a powerful technique for finding the best solutions for nonlinear systems. The mechanism adopted by this algorithm is that each particle is equivalent to an individual bird in a set of bids, which includes a swarm of N-particles moving around the d dimensional search space. An PSO algorithm can find the best

solutions through continuous updating of the search process, each particle swarm has an arbitrary speed, where the movement of each swarm of particles varies according to the best solutions that belong to it and its previous solutions in each iteration, Pbest (candidate solutions, local minima) and fitness values are stored in each particle's memory in the population. Gbest has the lowest fitness value of all the possible particles (global minima) [17] [18].

A PSO algorithm can be implemented using eq. (4) and (5),

$$V_i(k + 1) = w * V_i(k) + C_1 * r_1 * (P_i(k) - X_i(k)) + C_2 * r_2 * (P_g(k) - X_i(k)) \quad (4)$$

$$X_i(k + 1) = X_i(k) + V_i(k + 1) \quad (5)$$

where i is the particle's number, k is an iteration number, $V_i(k)$ is the moving velocity, $P_i(k)$ is Pbest, $P_g(k)$ is Gbest, $X_i(k)$ is the state of the i th particle, w is its inertia weight, r_1 and r_2 are random values, which are uniformly distributed random numbers in $[0, 1]$, it is important to know that these values are randomly generated and they may change during each iteration, C_1 and C_2 are constants which represent the control parameters of the PSO algorithm [19]. Figure 5 illustrates the PSO flowchart.

The PSO algorithm's objective is to determine the controller parameters in this study. FO-PID is more difficult to design because it contains five parameters ($K_p, K_i, K_d, \lambda, \mu$) and each of these parameters requires a process of adjustment and optimization when used in the required fields; however, the IO-PID controller only has three parameters (K_p, K_i, K_d), so tuning and optimizing these parameters is simpler than with the FO-PID controller compared to the IO- PID one [13].

To illustrate this process; Fig. 6 shows the block diagram of the IO-PID and FO-PID controllers with the PSO algorithm.

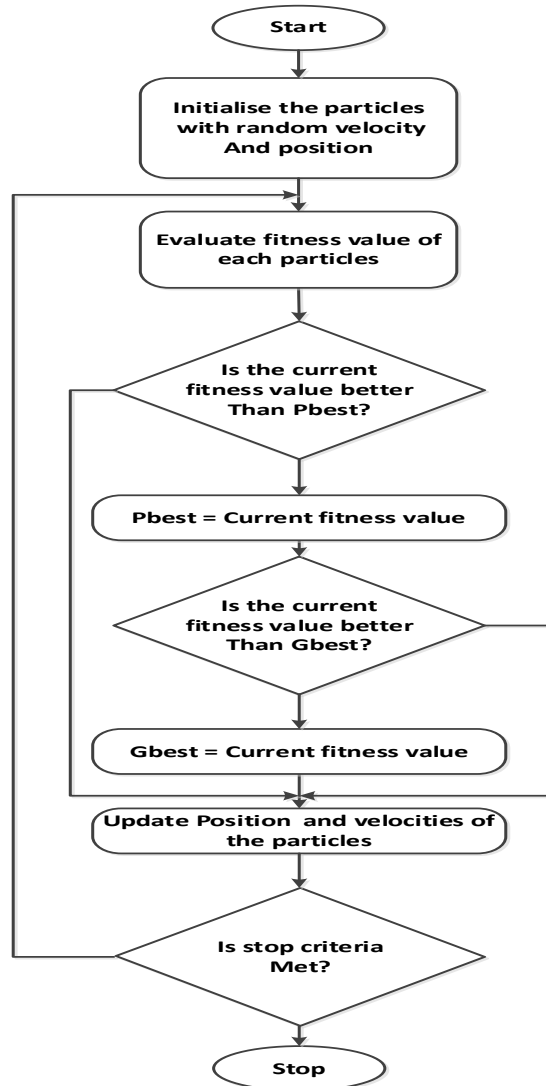


Figure 5 PSO flowchart.

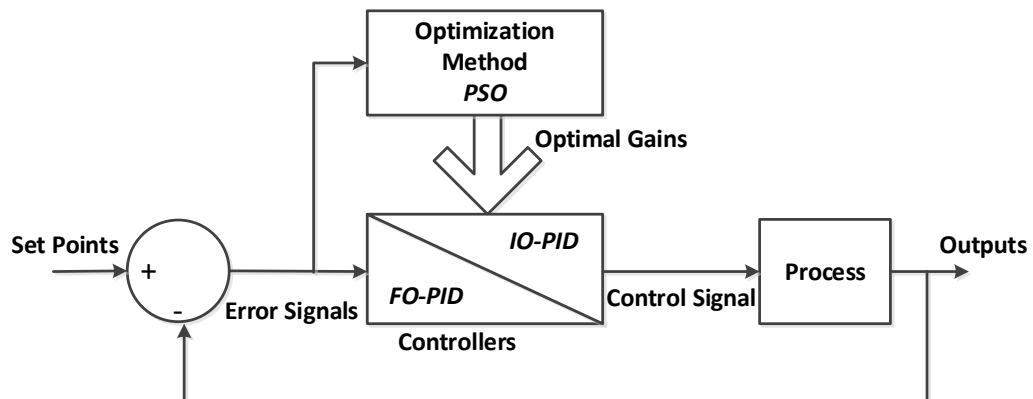


Figure 6 Block diagram of the PSO with FO-PID and IO-PID controllers.

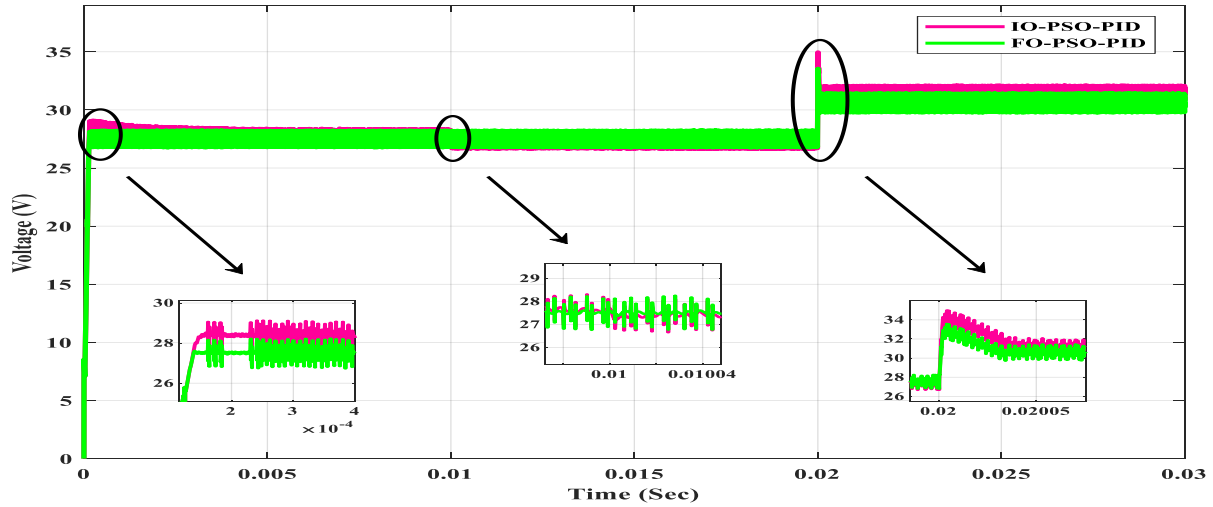
5. Simulations and Results:

The simulations are developed in the Simulink/MATLAB environment. The ESG's primary components are a DC-DC converter, H-bridge inverter, and a high-frequency transformer. Three load models are used to depict the impedance of tissues (Child, Male, and Female). The impedance of child tissue is composed of three layers, but the impedance of men and women is composed of four layers each. To optimize the IO-PID and FO-PID parameters for ESG system control, PSO techniques are used, and through which the best values for the parameters of the two types of controllers are obtained, Table. 4 shows the values for the parameters IO-PID and FO-PID that are obtained by applying an PSO algorithm.

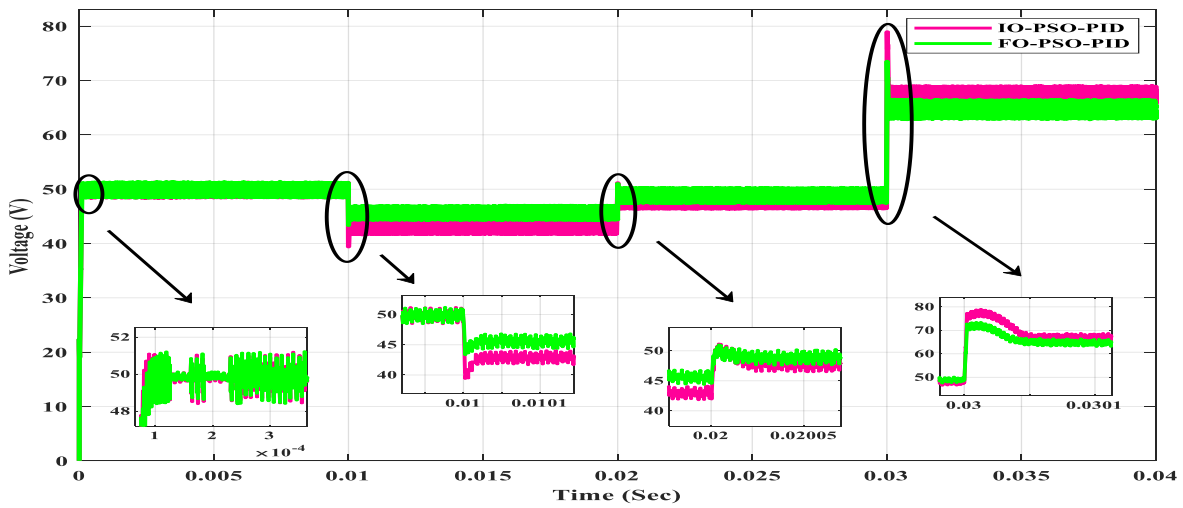
Table 4 Particle swarm optimization-PID controller parameters.

Description	IO-PID			FO-PID		
	Child	Male	Female	Child	Male	Female
Power loop						
K_p	3.500	4.8409	9.7722	3.0088	3.000	2.9300
K_i	2764.4472	86.7062	63.8989	3.3704	5.3007	5.2295
K_d	1.6829e-05	1.7170e-05	1.6632e-05	0.0607e-05	1.701e-05	6.9818e-05
λ	Not required	Not required	Not required	0.8688	0.9740	0.9159
μ	Not required	Not required	Not required	0.7532	0.0600	0.8062
Voltage loop						
K_p	0.6800	0.0979	0.0319	1.5790	2.8630	0.690
K_i	0.8747	0.6090	0.3242	3.8667	1.1401	0.4854
K_d	1.0489e-07	8.2703e-08	6.0214e-08	0.4603e-05	1.9964e-05	3.4160e-05
λ	Not required	Not required	Not required	0.9690	0.9280	0.7563
μ	Not required	Not required	Not required	0.637	0.9984	0.6398

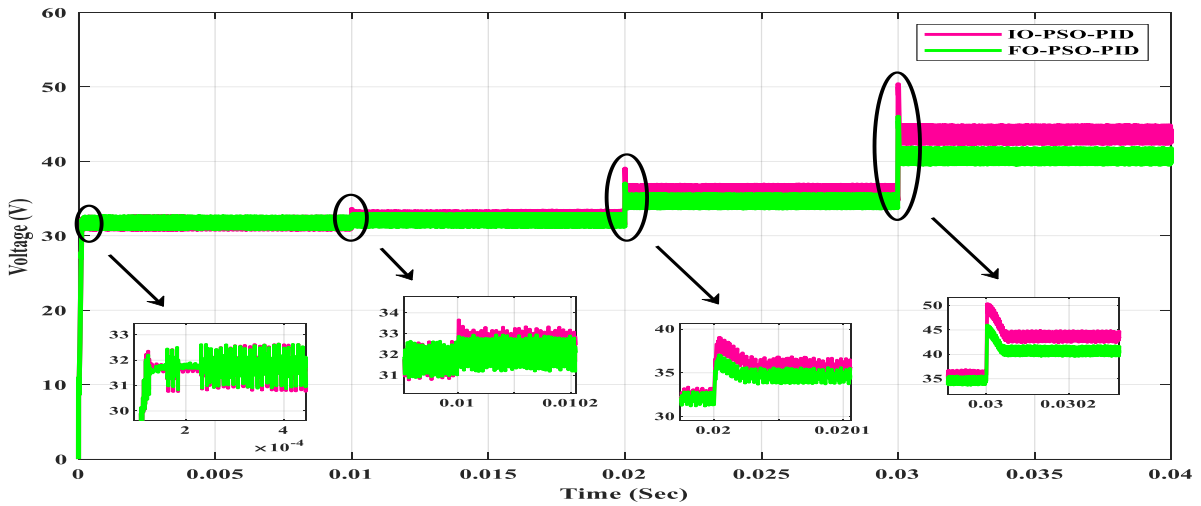
It should be noted that the loads handled (vital tissue) are loads that are variable in their impedance and not fixed. In addition, a detailed study is carried out for each of the layers of tissues for the three loads. From an applied point of view, computer simulations are shown in Fig. 7 which shows the output response behavior of voltage, current, and power of the ESG, the selected regions shown in Fig. 7, each region represent a layer of tissue layers, which is determined by the state of the transient behavior of the closed-loop ESG using the controllers IO-PID and FO-PID.



Child

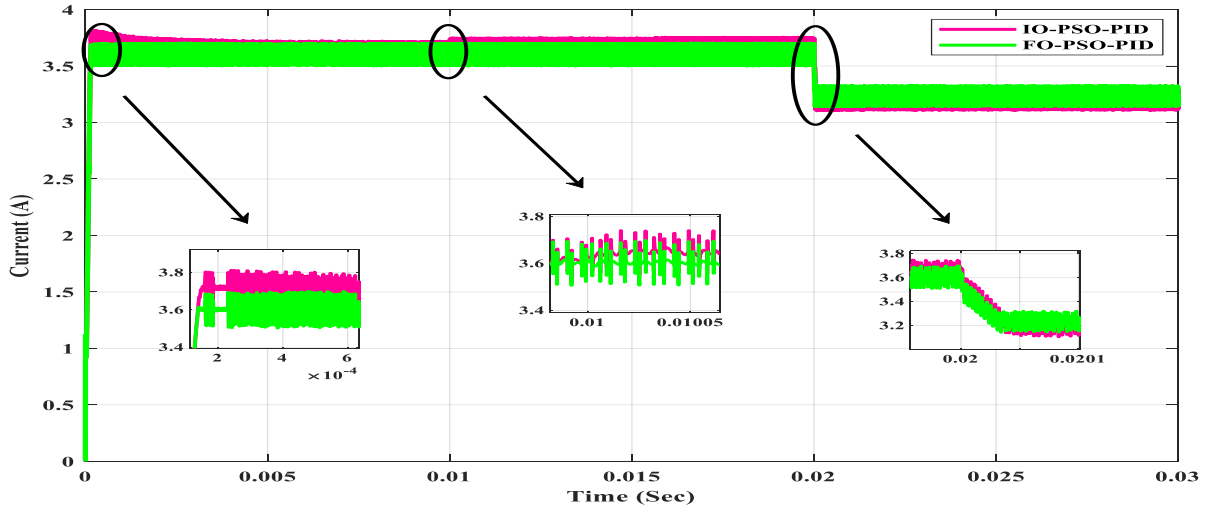


Male

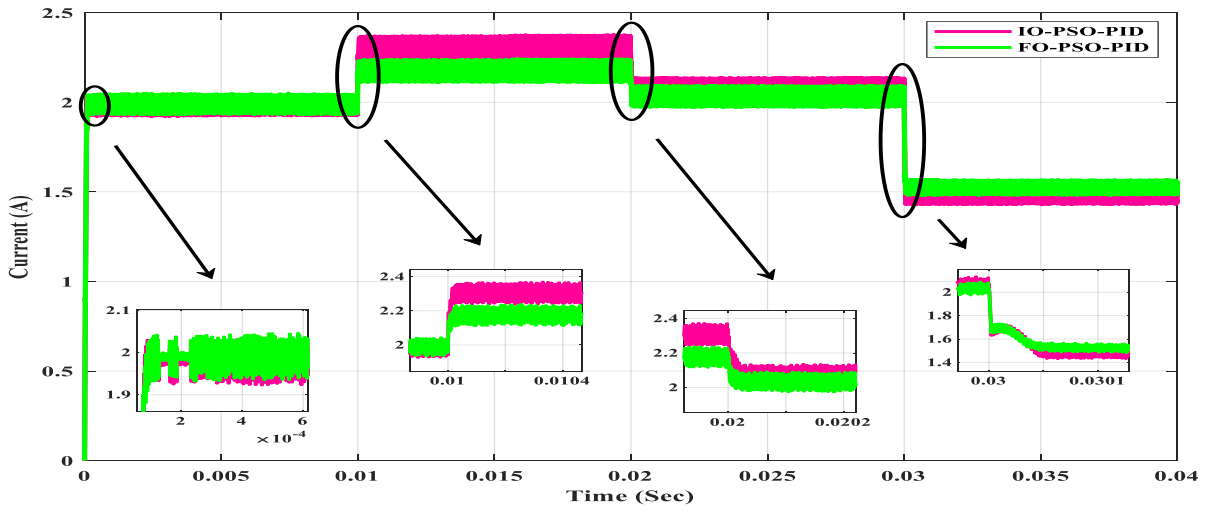


Female

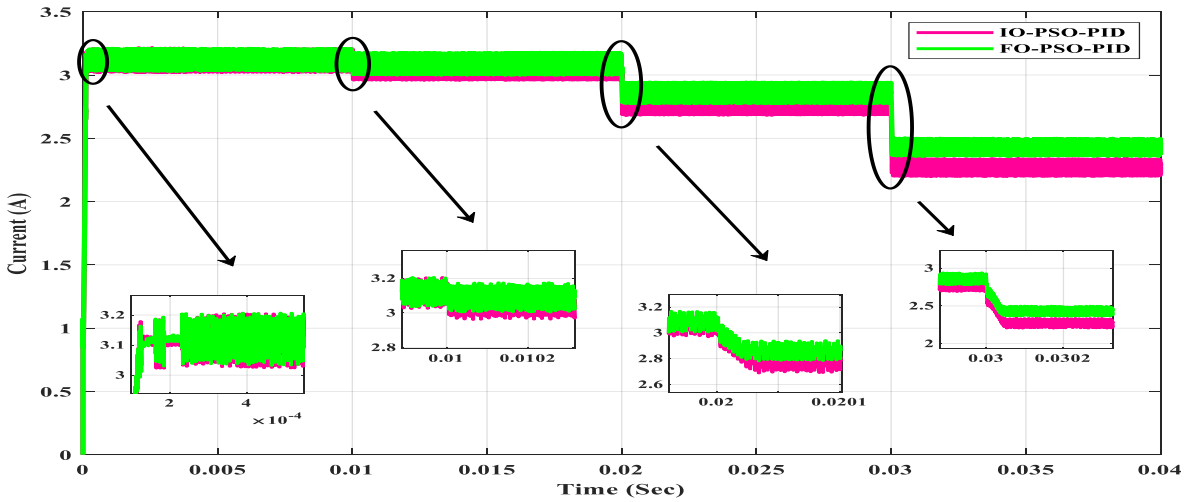
(a) Voltage (V)



Child

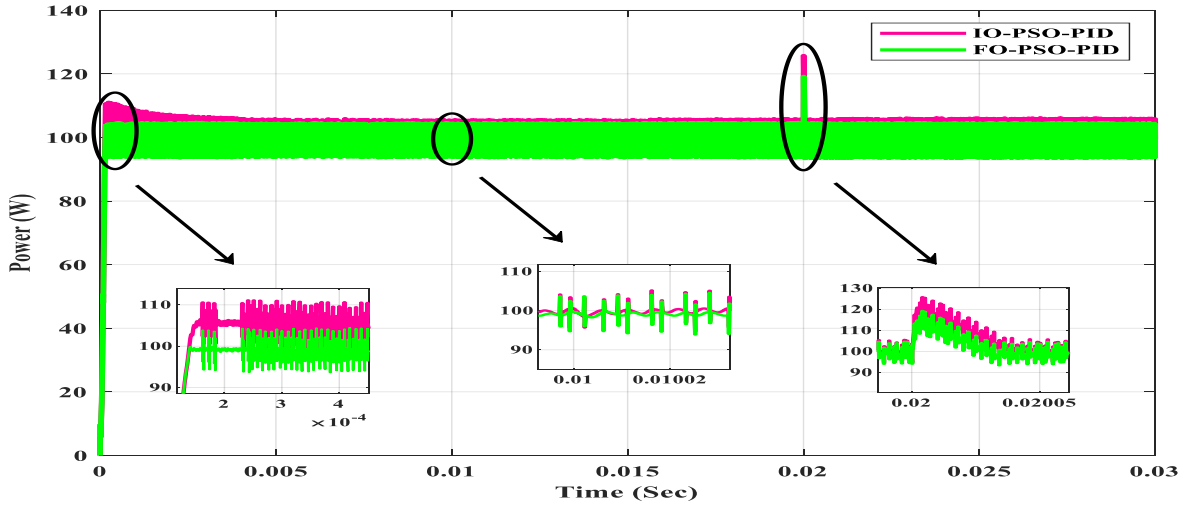


Male

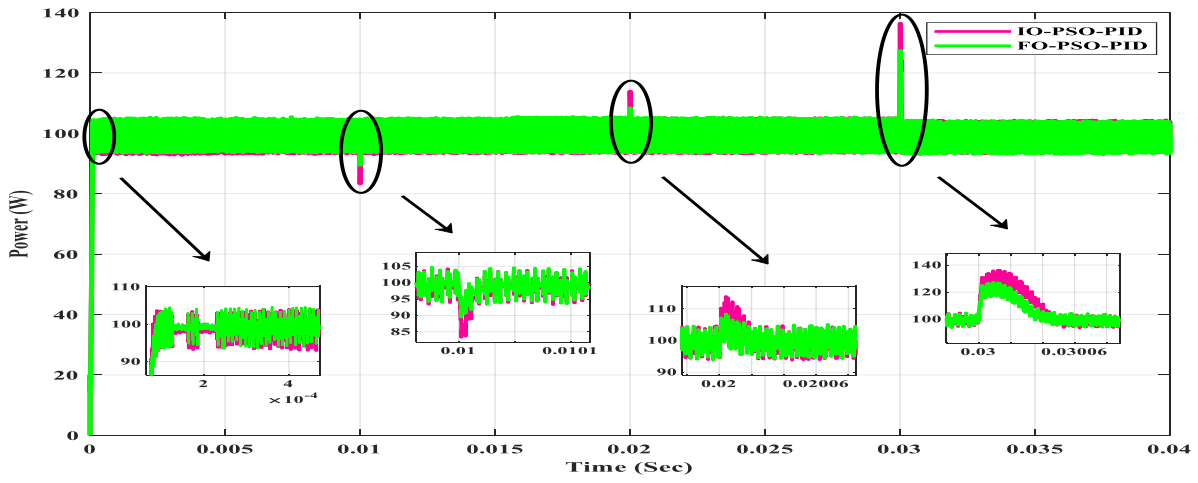


Female

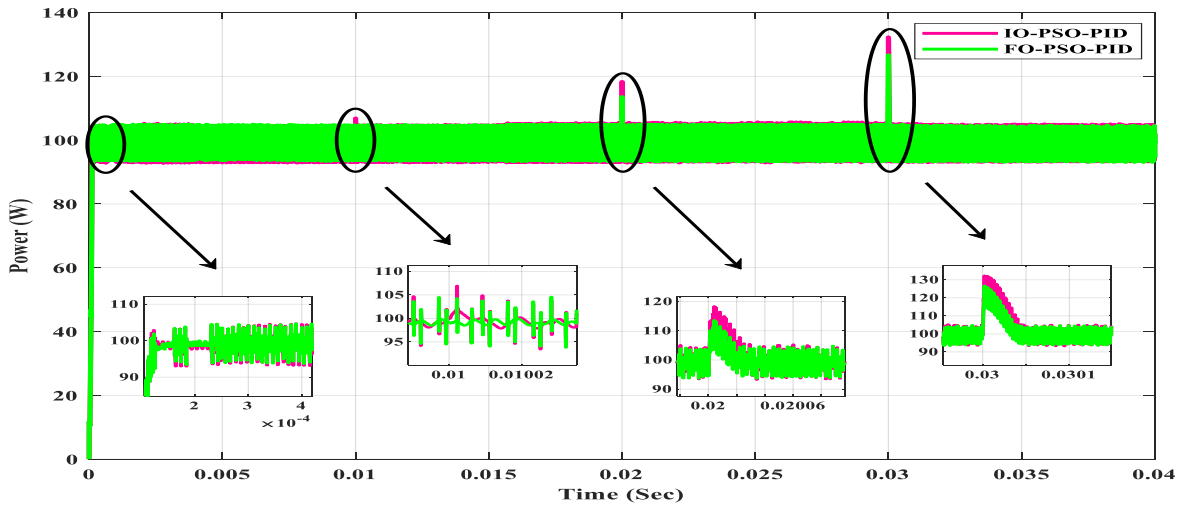
(b) Current (A)



Child



Male



Female

(c) Power (W)

Figure 7 Output Power, Voltage (RMS), Current (RMS) of ESG.

Based on research [6], the time taken to move from one layer to another during the cutting process is determined at about 0.01 Sec to perform the necessary clinical effects, and the relay is used as a switch to control the transition time for tissue layers. Based on this and through Fig. 7 it is clear that the transient state of the first layer is when the time is almost zero (the start of the ESG operation), and for the second layer it is at the time 0.01 Sec and the third layer is at the time 0.02 Sec, for the three loads (Child, Male, Female), and the fourth layer when the time 0.03 Sec for the two loads (Male, Female). From Fig. 7 (a), it can be seen clearly that the maximum amount of the output voltage of the ESG for the transient states to the layers of tissues (that is at the periods (0,0.01,0.02) Sec for the load that represents the child and (0,0.01,0.02,0.03) Sec when the load is the man or the woman), is the highest amount when using the controller IO-PID, if the comparison with the same figure using the controller FO-PID, and on the contrary in the case of the minimum amount of voltage, as finds that the magnitude in the case of using the controller IO-PID is less valuable from voltage amount when using FO-PID controller. The details mentioned above, regarding the output voltage of the ESG, also apply to the behavior of the output current of the ESG, which is shown in Fig.7 (b) and for all loads. On the theoretical level, a detailed comparison of the output of each of the generator voltage and current is included in the Table. 5, as the Table. 5 shows a comparison of the arithmetic values that were explained above and their clarification is represented in Fig. 7 (a) and (b).

Table 5 Comparison of voltage and current specification of the control system.

Description	IO-PID				FO-PID			
	Child				Child			
	Layer1	Layer 2	Layer 3	Layer 3	Layer1	Layer 2	Layer3	Layer3
Maximum Output Voltage (V)	29.18	28.39	35.08	35.08	28.23	27.98	33.58	33.58
Minimum Output Voltage (V)	0	26.97	30.50	30.50	0	26.83	29.86	29.86
Maximum Output Current (A)	3.82	3.74	3.32	3.32	3.70	3.68	3.28	3.28
Minimum Output Current (A)	0	3.61	3.19	3.19	0	3.55	3.13	3.13
Maximum Output Power (W)	110.50	105.14	125.03	125.03	104.28	104.45	119.47	119.47
Minimum Output Power (W)	0	94.31	93.15	93.15	0	96.03	93.47	93.47
	Male				Male			
	Layer1	Layer 2	Layer 3	Layer 4	Layer1	Layer 2	Layer3	Layer4
Maximum Output Voltage (V)	51.47	46.50	51.22	78.69	51.34	43.49	51.08	75.19
Minimum Output Voltage (V)	0	43.545	47.86	65.45	0	39.43	44.89	63.81
Maximum Output Current (A)	2.04	2.37	2.15	1.57	2.03	2.22	2.09	1.50
Minimum Output Current (A)	0	2.23	2.03	1.48	0	2.07	1.97	1.45
Maximum Output Power (W)	105.26	104.69	115.31	136.03	104.67	104.00	109.87	128.76
Minimum Output Power (W)	0	83.50	93.38	93.26	0	88.16	93.94	93.85
	Female				Female			
	Layer1	Layer2	Layer3	Layer4	Layer1	Layer2	Layer3	Layer4
Maximum Output Voltage (V)	32.70	33.67	39.01	50.37	32.65	32.93	37.13	46.51
Minimum Output Voltage (V)	0	32.45	34.78	42.34	0	30.88	33.76	39.50

Maximum Output Current (A)	3.21	3.18	3.09	2.86	3.21	3.10	2.86	2.85
Minimum Output Current (A)	0	2.95	2.74	2.20	0	3.06	2.83	2.35
Maximum Output Power (W)	105.69	106.72	118.55	132.33	104.62	104.58	113.73	126.74
Minimum Output Power (W)	0	93.10	92.92	93.08	0	93.60	93.39	93.15

The performance of IO-PID and FO-PID controllers inactive power control for ESG is depicted in Fig. 7 (c), it can see that the output power remains constant at 100 watts and that it is tracking the reference power (the desired amount that determined by the surgeon) regardless of the load's changing impedance tissues, where current and voltage are modified following the layer impedance of each load model as shown in Fig. 7 (a) and (b). Fig.7 (c) shows that the overshoot, as well as the undershoot, are decreases for all layers of the three loads when FO-PID is used as compared with the response performance shown by IO-PID, to explain it better, a detailed comparison is listed of the output power of the ESG characteristics using the controllers IO-PID and FO-PID in the Table. 6.

Table 6 Comparison of time-domain specification of the control system.

TIME DOMAIN SPECIFICATION	IOPID				FOPID			
	Child				Child			
	Layer1	Layer 2	Layer 3		Layer1	Layer 2	Layer3	
Overshot OS (%)	10.50	5.14	25.03		4.28	4.45	19.47	
Rising times Tr (μs)	97.02	97.02	97.43		95.26	95.77	95.40	
Settling times Ts(μs)	17.86	12.83	40.57		17.14	12.03	40.22	
Steady-state errors Ess (%)	0.69	0.62	0.28		0.08	0.13	0.01	
Undershoot US (%)	0	5.69	6.89		0	3.97	6.15	
	Male				Male			
	Layer1	Layer 2	Layer 3	Layer 4	Layer1	Layer 2	Layer3	Layer4
Overshot OS (%)	5.26	4.69	15.31	36.03	4.67	4.00	9.87	28.76
Rising times Tr (μs)	73.19	73.18	73.18	73.19	73.17	73.16	73.15	73.16
Settling times Ts (μs)	12.83	25.49	30.71	60.7	12.20	25.03	30.31	60.45
Steady-state errors Ess (%)	1.47	0.75	0.15	0.25	0.09	0.47	0.01	0.17
Undershoot US (%)	0	16.5	6.62	6.74	0	11.84	6.06	6.05
	Female				Female			
	Layer1	Layer2	Layer3	Layer4	Layer1	Layer2	Layer3	Layer4
Overshot OS (%)	5.69	6.72	18.55	32.33	4.62	4.58	13.73	26.74
Rising times Tr (μs)	109.30	110.28	109.30	109.30	107.20	109.29	107.19	107.19
Settling times Ts (μs)	15.66	15.46	40.48	50.89	15.49	15.11	40.25	50.45
Steady-state errors Ess (%)	0.34	0.63	0.52	0.56	0.09	0.31	0.31	0.16
Undershoot US (%)	0	6.75	7.08	6.92	0	6.04	6.61	6.85

Table. 6 shows the characteristics (overshoot, undershoot, rise time, settling time, steady-state error) of the ESG output power. The distinguished performance of FO-PID is not only limited to improving the overshoot and the undershoot but also contributes to reducing the time (rise time and

settling time) to ESG response. Reducing the time of rising time means to speed the response of the output power to reach the target point of the value determined by the surgeon, and the importance of this reduction is not hidden in helping to reduce the exposure of the target tissues to the electric power for a longer period, and in the same regard, reducing the settling time means reducing the continuation of the transient state of the output power of the ESG that is shed on the target tissues. Based on the above, the reduction that occurs in the time has a positive effect on the patient, as the short time that the power is needed for the necessary clinical procedure to take place on the target tissues, helps to reduce injuries, including burns harmful to the patient, which occurs due to the nature of the changing impedance to tissues, and this is one of the most important goals that it seeks to achieve most of the scientific studies specialized in this field, including this study. In addition, it should be noted that the decrease in the error rate of the ESG output power that is measured in the steady-state, which is between the reference value to be achieved and the measured value out of the ESG, is achieved by FO-PID if it is compared with the values obtained from using IO-PID, and this is shown in Table. 6.

Finally, it is concluded based on the simulation results shown by the comparison between IO-PID and FO-PID, that the last controller is characterized by a better performance in terms of contributing to reducing the percentage of overshoot (OV)%, undershoot (US)%, and steady-state error (ESS)%, as well as the time duration of rising time (T_r) Sec and settling time (T_s) Sec when it is compared with the results shown by the performance of the controller IO-PID.

6. CONCLUSIONS

In this work, it is proposed to implement the closed-loop system of the ESG to improve its performance and obtain an advanced ESG with high efficiency in its work. To regulate the output power of the ESG, it is proposed to use two types of controllers that are IO-PID and FO-PID. A detailed comparison was made for the effect of the controls on the closed-loop of the generator, which was tested on three different loads, as well as the discussion of the results obtained, where the results showed that choosing the controller IO-PID could not be considered a suitable option to improve the ESG characteristics. After presenting a detailed analysis for each of the control units studied in this study and based on the results obtained, it can be concluded that the ESG equipped with a type FO-PID control unit is more powerful and more efficient when compared with an ESG equipped with a type control unit IO-PID.

References:

- [1] M. A. K. El-Shafei, M. I. El-Hawwary, and H. M. Emara, "Implementation of fractional-order *PID* controller in an industrial distributed control system," in *2017 14th International Multi-Conference on Systems, Signals and Devices, SSD 2017*, Dec. 2017, vol. 2017-January, pp. 713–718. doi: 10.1109/SSD.2017.8167004.
- [2] Z. Bingul and O. Karahan, "Comparison of *PID* and *FOPID* controllers tuned by *PSO* and *ABC* algorithms for unstable and integrating systems with time delay," *Optimal Control Applications and Methods*, vol. 39, no. 4, pp. 1431–1450, Jul. 2018, doi: 10.1002/oca.2419.
- [3] A. A. Dastjerdi, N. Saikumar, and S. H. HosseinNia, "Tuning guidelines for fractional order *PID* controllers: Rules of thumb," *Mechatronics*, vol. 56, pp. 26–36, Dec. 2018, doi: 10.1016/j.mechatronics.2018.10.004.
- [4] M. Zamani, M. Karimi-Ghartemani, N. Sadati, "FOPID Controller Design for Robust Performance Using Particle Swarm Optimization," *Japanese J. Gastroenterol. Surg.*, vol. 30, no. 6, pp. 1391–1425, 1997, doi: 10.5833/jjgs.30.1391.
- [5] S. Fahad, N. Ullah, A. J. Mahdi, and N. Ullah, "A new robust closed-loop control system for electrosurgical generators," *Research on Biomedical Engineering*, vol. 36, no. 3, pp. 213–224, Sep. 2020, doi: 10.1007/s42600-020-00062-y.
- [6] A. M. Ridha, A. J. Mahdi, J. K. Abed, and S. Fahad, "*PID* fuzzy control applied to an electrosurgical unit for power regulation," *Journal of Electrical Bioimpedance*, vol. 11, no. 1, pp. 72–80, Jan. 2020, doi: 10.2478/joeb-2020-0011.
- [7] S. NasimUllah, M. M. Rafiq, M. Ishfaq, M. Ali, A. Ibeas, and J. Herrera, "A closed loop robust control system for electrosurgical generators," in *Control Applications for Biomedical Engineering Systems*, Elsevier Inc., 2020, pp. 149–168. doi: 10.1016/B978-0-12-817461-6.00006-8.
- [8] H. Saber, A. Jafer Mahdi, M. Hussein Nawir, S. Fahad, M. Shahzad Nazir, and A. Goudarzi, "Status: In Production Title: Investigation and Testing of High-Frequency open-loop Electrosurgical Generator under Varying Bio-tissue Impedances."

- [9] V. T. Tomov, "Modern Advances in Energy Based Electrosurgical Devices." [Online]. Available: <https://www.researchgate.net/publication/328773030>
- [10] S. Aminimoghaddam, R. Pahlevani, and M. Kazemi, "Electrosurgery and clinical applications of electrosurgical devices in gynecologic procedures," *Medical Journal of the Islamic Republic of Iran*, vol. 32, no. 1. Iran University of Medical Sciences, pp. 1–6, 2018. doi: 10.14196/mjiri.32.90.
- [11] K. Charoenkwan, Z. Iheozor-Ejiofor, K. Rerkasem, and E. Matovinovic, "Scalpel versus electrosurgery for major abdominal incisions," *Cochrane Database of Systematic Reviews*, vol. 2017, no. 6, Jun. 2017, doi: 10.1002/14651858.CD005987.pub3.
- [12] F. C. Meeuwssen, A. C. P. Guédon, E. A. Arkenbout, M. van der Elst, J. Dankelman, and J. J. van den Dobbelsteen, "The Art of Electrosurgery: Trainees and Experts," *Surgical Innovation*, vol. 24, no. 4, pp. 373–378, Aug. 2017, doi: 10.1177/1553350617705207.
- [13] M. Dulău, A. Gligor, and T. M. Dulău, "Fractional Order Controllers Versus Integer Order Controllers," in *Procedia Engineering*, 2017, vol. 181, pp. 538–545. doi: 10.1016/j.proeng.2017.02.431.
- [14] S. Fahad, N. Ullah, A.J. Mahdi, A. Ibeas, A. Goudarzi "An Advanced Two-Stage Grid Connected PV System: A Fractional-Order Controller," 2019.
- [15] A. T. Mohamed, M. F. Mahmoud, R. A. Swief, L. A. Said, and A. G. Radwan, "Optimal fractional-order PI with DC-DC converter and PV system," *Ain Shams Engineering Journal*, vol. 12, no. 2, pp. 1895–1906, Jun. 2021, doi: 10.1016/j.asej.2021.01.005.
- [16] J. Zhong and L. Li, "Tuning fractional-order PI λ D μ controllers for a solid-core magnetic bearing system," *IEEE Transactions on Control Systems Technology*, vol. 23, no. 4, pp. 1648–1656, Jul. 2015, doi: 10.1109/TCST.2014.2382642.
- [17] D. Wang, D. Tan, and L. Liu, "Particle swarm optimization algorithm: an overview," *Soft Computing*, vol. 22, no. 2, pp. 387–408, Jan. 2018, doi: 10.1007/s00500-016-2474-6.
- [18] S. Fahad, A. J. Mahdi, W. H. Tang, K. Huang, and Y. Liu, "Particle Swarm Optimization Based DC-Link Voltage Control for Two Stage Grid Connected PV Inverter," in *2018 International Conference on Power System Technology, POWERCON 2018 - Proceedings*, Jan. 2019, pp. 2233–2241. doi: 10.1109/POWERCON.2018.8602128.

- [19] A. J. Mahdi, W. H. Tang, and Q. H. Wu, "Parameter Identification of a PMSG Using a *PSO* Algorithm Based on Experimental Tests."

تحليل مقارن للمسيطر التناسبي-التكاملي-التفاضلي ذات الترتيب الصحيح والكسري لتنظيم قدرة مولد الجراحة الكهربائية

الخلاصة: يجب التحكم بالقدرة الخارجة من وحدة المولد الكهربائي للجراحة (*ESG*) بسبب عدم السيطرة على ممانعة الأنسجة أثناء العمليات الجراحية. تؤدي تغييرات ممانعة أنسجة الجلد إلى تعقيد أنظمة السيطرة على الجهد وذلك لتحقيق قدرة خارجية ثابتة. تهدف هذه الدراسة إلى التحكم الأمثل بالقدرة الخارجة ولأنواع مختلفة من الأنسجة حسب الجنس والعمر. يتم تمثيل أنسجة المعاوقة كدائرة *RC* موازية بثلاثة نماذج (طفل ، ذكر ، وأنثى). لتعزيز أداء المولدات الكهربائية الجراحية، تم تصميم وحدات تحكم *PID* ذات الترتيب الصحيح (*IO-PID*) و (*FO-PID*) ذات الترتيب الكسري من أجل التحكم بالقدرة والجهد الخارجيين. تُستخدم خوارزمية تحسين سرب الجسيمات (*PSO*) لتحسين معاملات وحدات التحكم *IO-PID* و *FO-PID*. تم مقارنة نظامي التحكم اعتماداً على معاملات الأداء التقليدية (أعلى وأدنى قدرة مستهلكة في الحالة العابرة إضافة إلى زمن الاستقرار)، وخلص إلى أن *ESG* القائم على *FO-PID* هو أكثر متانة وكفاءة مقارنة مع *ESG* القائم على *IO-PID*.